



## CRISPR/Cas9 mediated knockout of the *abdominal-A* homeotic gene in the global pest, diamondback moth (*Plutella xylostella*)



Yuping Huang<sup>a, b, c</sup>, Yazhou Chen<sup>d</sup>, Baosheng Zeng<sup>d</sup>, Yajun Wang<sup>a, b, c</sup>,  
 Anthony A. James<sup>e, f</sup>, Geoff M. Gurr<sup>a, b, c, g</sup>, Guang Yang<sup>a, b, c</sup>, Xijian Lin<sup>a, b, c</sup>,  
 Yongping Huang<sup>d, \*\*</sup>, Minsheng You<sup>a, b, c, \*</sup>

<sup>a</sup> Institute of Applied Ecology, Fujian Agriculture and Forestry University, Fuzhou 350002, China

<sup>b</sup> Fujian-Taiwan Joint Centre for Ecological Control of Crop Pests, Fujian Agriculture and Forestry University, Fuzhou 350002, China

<sup>c</sup> Key Laboratory of Integrated Pest Management for Fujian-Taiwan Crops, Ministry of Agriculture, Fuzhou 350002, China

<sup>d</sup> Key Laboratory of Insect Developmental and Evolutionary Biology, Institute of Plant Physiology and Ecology, Shanghai Institutes for Biological Sciences, Chinese Academy of Sciences, Shanghai 200032, China

<sup>e</sup> Department of Microbiology & Molecular Genetics, University of California, Irvine, CA 92697-4025, USA

<sup>f</sup> Department of Molecular Biology & Biochemistry, University of California, Irvine, CA 92697-3900, USA

<sup>g</sup> Graham Centre, Charles Sturt University, Orange, NSW 2800, Australia

### ARTICLE INFO

#### Article history:

Received 22 February 2016

Received in revised form

14 June 2016

Accepted 14 June 2016

Available online 16 June 2016

#### Keywords:

Pest

Lepidoptera

Germline stability

Phylogenetic analysis

Gene mutation

### ABSTRACT

The diamondback moth, *Plutella xylostella* (L.), is a worldwide agricultural pest that has developed resistance to multiple classes of insecticides. Genetics-based approaches show promise as alternative pest management approaches but require functional studies to identify suitable gene targets. Here we use the CRISPR/Cas9 system to target a gene, *abdominal-A*, which has an important role in determining the identity and functionality of abdominal segments. We report that *P. xylostella abdominal-A* (*Pxabd-A*) has two structurally-similar splice isoforms (A and B) that differ only in the length of exon II, with 15 additional nucleotides in isoform A. *Pxabd-A* transcripts were detected in all developmental stages, and particularly in pupae and adults. CRISPR/Cas9-based mutagenesis of *Pxabd-A* exon I produced 91% chimeric mutants following injection of 448 eggs. Phenotypes with abnormal prolegs and malformed segments were visible in hatched larvae and unhatched embryos, and various defects were inherited by the next generation ( $G_1$ ). Genotyping of mutants demonstrated several mutations at the *Pxabd-A* genomic locus. The results indicate that a series of insertions and deletions were induced in the *Pxabd-A* locus, not only in  $G_0$  survivors but also in  $G_1$  individuals, and this provides a foundation for genome editing. Our study demonstrates the utility of the CRISPR/Cas9 system for targeting genes in an agricultural pest and therefore provides a foundation for the development of novel pest management tools.

© 2016 Elsevier Ltd. All rights reserved.

### 1. Introduction

The diamondback moth (DBM), *Plutella xylostella* (L.), is one of the most destructive and cosmopolitan pests of cruciferous crops. It attacks many economically important food crops such as oilseed rape and cabbage, and the annual total cost of damage and management worldwide is estimated at USD4–5 billion (Furlong et al.,

2013; Zalucki et al., 2012). *Plutella xylostella* has developed resistance to all major classes of pesticides, including dichlorodiphenyl-trichloroethane (DTT) and *Bacillus thuringiensis* (Bt) (Angkersmit, 1953; Johnson, 1953; Tabashnik et al., 1990), making it difficult to control and demanding the development of novel management strategies. Genetics-based technologies such as piggyBac-mediated transgenesis, support the ability to develop population-suppression DBM strains by release of insects carrying a dominant lethal trait (RIDL) (Martins et al., 2012). Although piggyBac is a versatile transposon element for engineering insects, its random integration, relatively low transforming frequency, possible instability of integrated sequences, and limited carrying capacity hamper its wide application in pest control trials (Fraser Jr,

\* Corresponding author. Institute of Applied Ecology, Fujian Agriculture and Forestry University, Fuzhou 350002, China.

\*\* Corresponding author.

E-mail addresses: [yphuang@sibs.ac.cn](mailto:yphuang@sibs.ac.cn) (Y. Huang), [msyou@iae.fjau.edu.cn](mailto:msyou@iae.fjau.edu.cn) (M. You).

2012).

CRISPR/Cas9 (clustered regularly interspaced short palindromic repeats (CRISPR)-associated protein) is a newly emerged genome-editing tool with advantages over the earlier, time- and labor-consuming techniques: zinc finger nucleases (ZFN) and transcription activator-like effector nucleases (TALENs) (Miller et al., 2007, 2011; Porteus and Baltimore, 2003; Sander et al., 2011; Wood et al., 2011). This novel methodology needs only the Cas9 nuclease coupled with a single guide RNA (sgRNA) to cleave a specific sequence. Since the first demonstration of engineering the type II CRISPR-Cas9 system to function in eukaryotes (Cong et al., 2013), the technique has been used to edit genomes of numerous species including human (cells), mice, nematodes (*Caenorhabditis elegans*) and insects (*Drosophila melanogaster*), and for substantially improving the ease of genome editing and studies of genome regulation (Cho et al., 2013; Friedland et al., 2013; Gilbert et al., 2013; Gratz et al., 2013; Li et al., 2013; Qi et al., 2013).

The *abdominal-A* (*abd-A*) gene, belonging to the homeotic gene (Hox) family, is a member of *Drosophila* bithorax complex, which is required for segmental identity during embryogenesis (Sánchez-Herrero et al., 1984). These genes encode transcription factors that modulate segment development by interacting with a large number of downstream target genes (Pavlopoulos and Akam, 2011). Gene products of *abd-A* are involved in many biological processes during early embryogenesis of *Drosophila* and other insects. These include the differentiation of the anterior body and rear somite axis, cardiac tube organogenesis, heart cell fate in the dorsal vessel, genesis of the nervous system and fat body, gonad formation and development, midgut formation and muscle patterning (Cumberledge et al., 1992; Foronda et al., 2006; Lovato et al., 2002; Marchetti et al., 2003; Mathies et al., 1994; Michelson, 1994; Perrin et al., 2004; Ponzielli et al., 2002). Products of *abd-A* also play a role in larva-to-pupa metamorphosis in the silkworm, *Bombyx mori*, and abdominal pigmentation of adult *D. melanogaster* (Deng et al., 2012; Rogers et al., 2014). RNAi of *abd-A* in silkworms results in complete or partial absence of ventral appendages (prolegs and legs) from the third to sixth abdominal segments in late-stage embryos, indicating its importance in the normal development of these segments (Pan et al., 2009).

We cloned the *P. xylostella* ortholog, designated *Pxabd-A*, profiled levels of expression across different life stages and sexes, and applied the CRISPR/Cas9 system to generate loss-of-function individuals and visible defect phenotypes. Severe abdominal morphological defects and significant lethality resulted from disruption of the gene. Our results demonstrate the possibility of further gene function studies based on genome editing and developing novel approaches for genetic control of this globally important pest insect.

## 2. Materials and methods

### 2.1. Experimental DBM strain

The experimental DBM strain (Fuzhou-S) was derived from insecticide-susceptible insects collected from a cabbage (*Brassica oleracea* var. *capitata*) crop in Fuzhou (26.08°N, 119.28°E) in 2004 and later used for genome sequencing (You et al., 2013). Larvae were reared on potted radish seedlings (*Raphanus sativus* L.) at 25 ± 1 °C, 65 ± 5%RH and L:D = 16:8 h, in a greenhouse without exposure to insecticides.

### 2.2. Cloning of *Pxabd-A*

Total RNA was isolated from five *P. xylostella* 3<sup>rd</sup> instar larvae using the TRIzol Reagent (Invitrogen, Carlsbad, CA, USA). First-

strand cDNA was synthesized with Hiscript™ Reverse Transcriptase (Vazyme Biotech) by using 500 ng total RNA. The *Pxabd-A* cDNA was amplified with a pair of primers (F: 5'- ATG AGT TCC AAG TTC ATC ATC G - 3'; R: 5'- TTA CGT GGG CAC CTT GTT GA - 3') corresponding to the predicted coding sequence of *Pxabd-A* (gene ID in DBM genome: Px004264) in the *P. xylostella* genome (<http://iae.fafu.edu.cn/DBM/index.php>). PCR was carried out with KOD-plus polymerase (TOYOBO, Japan) under the following conditions: 98 °C for 2 min, and then 30 cycles at 98 °C for 30 s, 55 °C for 30 s, 68 °C for 70 s, and a final elongation step at 68 °C for 10 min. PCR products were isolated on a 1% agarose gel stained with ethidium bromide. The target band was extracted using the Omega gel extraction kit (Omega) and cloned into PJET1.2 vector (Thermo scientific) for sequencing.

### 2.3. Alignment and phylogenetic analysis of *Pxabd-A*

Multiple alignments were conducted using the MUSCLE algorithm based on the amino acid sequences encode by *abd-A* orthologs from 12 species (*P. xylostella*; *B. mori*, *Bombus terrestris*, *Apis mellifera*, *Tribolium castaneum*, *Anopheles gambiae*, *Drosophila melanogaster*, *Acyrtosiphon pisum*, *Myrmica rubra*, *Strigamia maritima*, *Hymenolepis microstoma* and *Echinococcus granulosus*) available in GenBank. The phylogenetic tree was constructed using the maximum likelihood method with a bootstrap value of 1,000 in MEGA5.1.

### 2.4. Expression profiling of *Pxabd-A*

The quantitative reverse transcription (qRT)-PCR-based expression profiling of *Pxabd-A* was performed using cDNA samples of eggs, 1<sup>st</sup> and 2<sup>nd</sup> instar larvae, male and female 3<sup>rd</sup>/4<sup>th</sup> instar larvae, prepupae, pupae, and adults. qRT-PCR was performed using transcript-specific primers (*Pxabd-A*-qRT-F: 5'- GAA GGA GAT CAA CGA GCA GG -3', *Pxabd-A*-qRT-R: 5'- GTG GGC ACC TTG ACT TT -3'; isoform A-qRT-F: 5'- CCA TCA CTG ATT TTC CAT TTC CAG -3', isoform A-qRT-R: 5'- CGT CAG GTA GTG GTT GAA GTG GAA -3') for *Pxabd-A* and isoform A, respectively. SYBR Select Master Mix for CFX kit (Life Technologies) was used to conduct qRT-PCR under the conditions: 50 °C for 2 min, then 95 °C for 2 min, and 40 cycles at 95 °C for 15 s, 60 °C for 30 s. The *P. xylostella* ribosomal protein gene S64 was used as the reference (F: 5'- CAA TCA GGC CAA TTT ACC GC -3'; R: 5'- CTG GGT TTA CGC AGT TAC G -3').

### 2.5. *In vitro* transcription of Cas9 and sgRNA

A 23 base-pair (bp) sgRNA targeting site located at nucleotides 163–185 bp (5'- GGA CTG AGT GCA GCG GCT CTA GG -3') was selected in Exon I of *Pxabd-A*. The control sgRNA (5'- GGC GAG GGC GAT GCC ACC TA -3') was used to target the exogenous gene encoding the EGFP protein, and the targeted efficiency of EGFP-sgRNA verified in a DBM embryo cell line (established in our laboratory). The sgRNA was generated from a ready-to-use 500 bp linearized vector by annealing oligonucleotide duplexes encoding the 20 bp target sequence upstream of protospacer adjacent motif (PAM), with the sgRNA expressed under control of the T7 promoter. The sgRNA template was subcloned into the PJET1.2 vector (Fermentas, Ontario, CA) and sequenced to verify the structure. sgRNA was synthesized *in vitro* using the MAXIcript T7 kit (Ambion). The PTD1-T7-Cas9 vector (ViewSolid Biotech, Beijing, China) was linearized with the *NotI* restriction enzyme (Fermentas, US), and the Cas9 mRNA synthesized *in vitro* using the mMESSAGE mMACHINE T7 Kit (Ambion).

## 2.6. Embryo microinjection

Female *P. xylostella* adults were caged to allow oviposition on 10 cm<sup>2</sup> parafilm sheets treated previously with a cabbage leaf extract. The sheets were renewed at intervals of 30 min to obtain fresh eggs. Eggs were aligned individually along the same anterior-posterior axis (Fig. S1) and microinjected with 300 ng/μl or 500 ng/μl of Cas9 mRNA along with 150 ng/μl sgRNA into the posterior pole of each egg within one hour of oviposition. Eggs were incubated at 25 °C.

## 2.7. Phenotype screening

Injected eggs were checked for development to calculate the hatching rate, and observed under a stereo microscope (Nikon, SW-2B/22) to examine the abdominal morphology of embryos on the third day after injection. Hatched larvae were observed under a microscope to detect mutated G<sub>0</sub> individuals that were subsequently reared on radish plants at 25 °C. The mutant phenotypes were imaged digitally with a stereo microscope.

## 2.8. T7 endonuclease I assay and characterization of targeted mutant loci

To confirm the mutagenesis of the *Pxabd-A* locus, genomic DNA from the 4<sup>th</sup> instar somatic mutants or wild-types was extracted individually (DNA extraction kit; CWBio, China). PCR was performed to amplify the fragments surrounding the sgRNA targeted sites from the genomic DNA samples using Phusion High-Fidelity DNA polymerase (New England Biolabs [NEB]) with *Pxabd-A* target site-specific primers (F: 5'-GCA GTT CCA TCA TCA GAA CTT G-3'; R: 5'-CAG TGA TGG ACA TCC AAG GAT A-3'). A hybridization reaction was run with 19 μl mixtures containing 200 ng of the PCR products, 2 μl NEB buffer 2 and ddH<sub>2</sub>O in a PCR cyclor: 95 °C for

5 min; ramping down with -2 °C/s to 85 °C and with -0.1 °C/s to 25 °C; and finally holding at 4 °C. The mixture then was treated with 1 μl of T7 endonuclease I (NEB) at 37 °C for 15 min and the reaction stopped by adding 2 μl of 0.25 M EDTA. The reaction mixture was resolved on a 2% agarose gel, and the DNA fragments analyzed under UV. The intensity of the fragments was quantified by Quantity one software (Bio-Rad, Hercules, California). PCR products of the mutants were ligated into pJET-Blunt vector and sequenced for validation of the genomic mutated events. Genomic DNA was prepared from 20 unhatched eggs to identify somatic mutations. The Gbdirect PCR kit (Genebank Biosciences Inc., China) was used to amplify potential mutated fragments. Amplified fragments were cloned into pJET1.2 (Fermentas, US) and sequenced.

## 3. Results

### 3.1. Identification and characterization of *Pxabd-A*

The *B. mori abd-A* ortholog, *Bmabd-A* (GeneBank EU365399), was used as a query with blastn to identify the putative coding sequence of *Pxabd-A* from the *P. xylostella* genome (You et al., 2013). *Pxabd-A* was mapped to region 991,463–1,151,462 bp in scaffold 17 of the genome. Analysis of the complete coding sequence showed that *Pxabd-A* has two splice isoforms, which we designate A and B (Fig. 1A). *Pxabd-A* isoform A contains three exons (604, 60, and 401 bp in length) and two introns (4,977 and 23,213 bp), for a total coding sequence of 1,065 bp. Isoform B differs from isoform A in the length of exon II (45 bp) and the first intron (4,992 bp), and has a coding sequence 1,050 bp in length. Our *abd-A* phylogenetic tree shows a clear pattern of order-specific clustering within the Insecta, supporting the conclusion that the corresponding genes are conserved within each of the groups (Fig. 1B). *Plutella xylostella* and *B. mori* are clustered into the Lepidoptera clade and are divergent from the Diptera clade represented by the mosquito, *Anopheles*

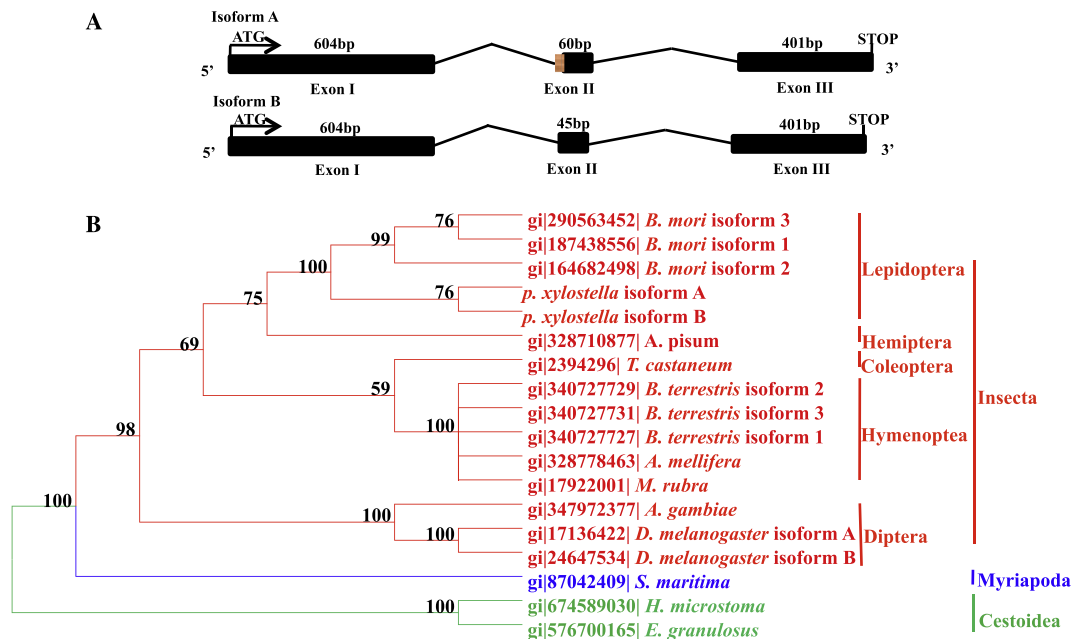


**Fig. 1. (A) Gene structure of the *P. xylostella abdominal-A* ortholog (*Pxabd-A*).** *Pxabd-A* has two isoforms (A and B), and both have three exons and two introns with similar primary structure. Numbers refer to the length in base-pairs (bp) of each gene component. ATG and STOP denote the translation initiation and termination codons, respectively. The orange block denotes the additional sequence present in Exon II of isoform A; **(B) Phylogenetic tree of *abd-A* based on the alignment of amino acid sequences of 12 species.** The tree involves three major branches: Insecta (nine species in red lettering), Myriapoda (one species in blue lettering) and Cestoidea (two species in green lettering). Support values are derived from 1,000 bootstrap replicates. Gene identification (gi) numbers are provided for each entry. (For interpretation of the references to colour in this figure legend, the reader is referred to the web version of this article.)

*gambiae*, and fruit fly, *D. melanogaster*. The isoforms are well-clustered in the insects (*P. xylostella*, *B. mori*, *B. terrestris* and *D. melanogaster*), supporting the conclusion that they result from a function-associated divergence within each species.

### 3.2. Expression profiling of *Pxabd-A*

Previous studies have established that *abd-A* transcripts are expressed in almost all abdominal segments during embryo development (Busturia et al., 1989; Peifer et al., 1987; Sánchez-Herrero et al., 1984). However, in later developmental processes, *abd-A* was acting downstream of the genes that define position and cell type within segments, as intermediates in the hierarchy of control that leads to morphogenesis (Foronda et al., 2006; LaBeau et al., 2009; Peifer et al., 1987). qRT-PCR-based expression profiling showed that total *Pxabd-A* (isoforms A and B), and isoform A transcript accumulation levels were lower in 1<sup>st</sup>-4<sup>th</sup> instar larvae and prepupae compared with the egg, pupa, and adult (Fig. 2). Eggs and adult female and male insects accumulated the transcripts to levels 10-fold higher than the larval stages. The highest abundance, ~15-fold greater than larval instars, was seen in female and male pupae. Isoform A exhibited the same level of transcript abundance between male/female pupae and adults. *Pxabd-A* transcripts accumulated were lower in female adults than male adults. Accumulation levels of isoform B transcripts were generally similar to isoform A, but higher in male adults compared with females (Fig. 2). Our finding that *Pxabd-A* was expressed in all developmental stages tested and both sexes provides a basis for further functional studies.

### 3.3. Phenotypes induced by disruption of *Pxabd-A*

To test the role of *Pxabd-A* in *P. xylostella*, a single target site in exon I of the *Pxabd-A* locus was selected for CRISPR/Cas9 mutagenesis (Fig. 4A). We injected *Pxabd-A*-sgRNA or EGFP-sgRNA (control) along with Cas9 mRNA into preblastoderm embryos. In the groups treated with *Pxabd-A* sgRNA, loss-of-function mutations of *Pxabd-A* were induced with a higher efficiency (91%) when injected with 500 ng/μl Cas9 mRNA when compared with

injections of 300 ng/μl (35%) (Table 1). Injection of structurally unrelated sgRNA for the EGFP control did not affect development of embryos and larvae. Hatchability of eggs was relatively low in the *Pxabd-A* specific sgRNA treatment. We checked individual unhatched eggs to determine if there was a visible phenotypic effect of *Pxabd-A* sgRNA. Some of the eggs developed sufficiently to form the black head capsule indicative of larvae (Fig. S2A), while 82 individual unhatched embryos exhibited a severe abdominal distortion (Fig. S2B). Most unhatched eggs from the EGFP-sgRNA injected control exhibited yellow coloration, possibly because of microinjection damage. The developing embryos with black head capsules had normal segmentation and prolegs. A total of 218 pupae (90%) developed and produced adults in the EGFP-sgRNA control, a rate similar to that reported for the wild-type (Peng et al., 2015).

In the *Pxabd-A*-sgRNA treatment, excluding the 82 mutated unhatched eggs, 281 of the 501 injected eggs hatched and produced larvae with mutant phenotypes in which abdominal segments were fused (Fig. 3A and B) and 189 of these died within two days. A total of 92 larvae with less-severe mutations survived to the 4<sup>th</sup> instar stage (Fig. 3C) and 73 of these pupated (Fig. 3D). Insects resulting from the CRISPR targeted *Pxabd-A* locus could be divided into two classes based on loss-of-function phenotypes. The first class had larval phenotypes with fused abdominal segments (Fig. 3B), crochets absent from some prolegs (Fig. 3E) or deformed testis (Fig. 3F). The larvae with segment defects could walk only with their thoracic legs (Movie 1), and died within two days. The second class comprised adult phenotypes with external genitalia deviating from the central axis (Fig. 4A) and deformed testis (Fig. 4B). Of the 23 males, 21 (91%) were sterile. In the mutated G<sub>0</sub>, 57% of the female adults layed eggs. Sterile females that layed no eggs despite the presence of eggs in the ovary may have resulted from normal egg migration being disrupted as reported for the phenotypes from different mutations of *abd-A* in *Drosophila* (Cumberledge et al., 1992). It appears that sterility is caused, at least in part, by the disruption of gonad development induced by CRISPR/Cas targeting of *Pxabd-A* locus. Collectively these two classes of phenotypes support the interpretation *Pxabd-A* may play a largely permissive role in promoting segmentation and gonad development in the

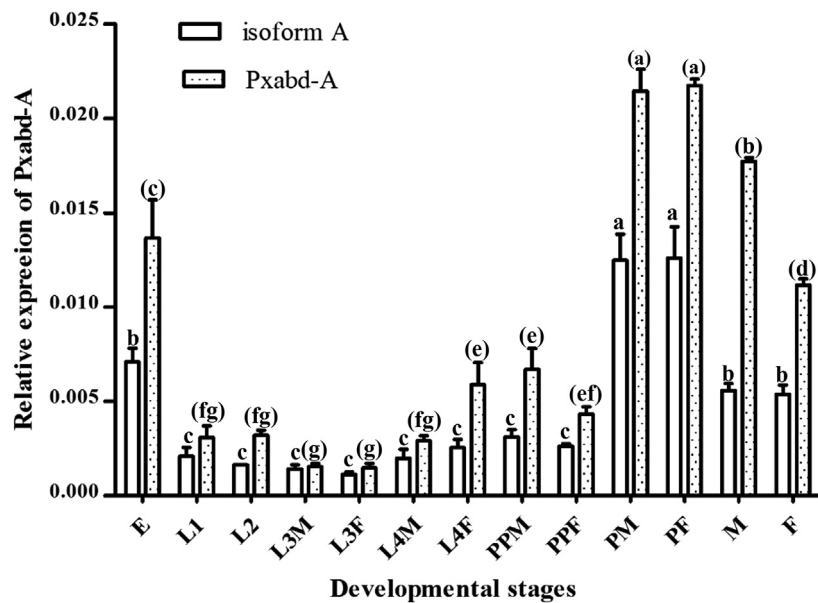


**Fig. 2.** qRT-PCR-based expression of *Pxabd-A* at different developmental stages and sexes of the adult. Abbreviations: E, eggs; L1, L2 represent 1<sup>st</sup>, 2<sup>nd</sup> instar larvae; L3M, L3F, L4M and L4F represent 3<sup>rd</sup> and 4<sup>th</sup> male/female instar larvae, respectively; PPM and PPF represent male and female prepupae; PM and PF represent male and female pupae; M and F represent male and female adults. Error bars indicate standard errors of the mean. Statistically-significant differences were labeled with different letters or letters in parentheses as analyzed with one-way ANOVA (Duncan's multiple range test,  $P < 0.05$ ,  $n = 3$ ).



**Table 1**  
Mutagenesis mediated by CRISPR/Cas9 targeted *Pxabd-A*<sup>a</sup>.

Concentration of Cas9 mRNA	sgRNA	Injected embryos	Hatchability	G <sub>0</sub> mosaic	Germline transmission rate
300 ng/μL	abd-A-sgRNA	337	62%	(81) 35%	0
	EGFP-sgRNA	242	68%	/	/
500 ng/μL	abd-A-sgRNA	448	57%	(282) 91%	9.1%
	EGFP-sgRNA	238	70%	/	/

<sup>a</sup> For each concentration, Cas9 mRNA with different sgRNAs (abd-A-sgRNA or EGFP-sgRNA) was injected into embryos. G<sub>0</sub> mosaic records the abnormal hatched larvae and dissected disorder unhatched eggs. The G<sub>0</sub> mutation rate = (mutated larvae + mutated unhatched eggs)/(hatched larvae + mutated unhatched eggs). The germline transmission rate = positive G<sub>1</sub> egg batches/G<sub>1</sub> egg batches. Each G<sub>1</sub> egg batch was from a different mutated G<sub>0</sub> parent (females and males). The positive G<sub>1</sub> egg batch indicates one and more offspring showing mutated phenotype and genotype. The germline transmission rate indicates the fraction of parents that produced one or more mutants in their germline.

diamondback moth.

Supplementary video related to this article can be found at <http://dx.doi.org/10.1016/j.ibmb.2016.06.004>.

#### 3.4. CRISPR/Cas9 mediated mutagenesis of *Pxabd-A*

Genomic DNA from unhatched egg was used as a template to amplify the sgRNA target region and confirm that unhatched mutated eggs were caused by mutagenesis of *Pxabd-A* locus. Four of six sequenced clones (66%) were found to have insertion and deletion mutations caused by CRISPR/Cas9-induced non-homologous end joining (Fig. 5C a). Furthermore, mutation events at the targeted region of the *Pxabd-A* locus in five randomly-

selected, mutated 4<sup>th</sup> instar larvae were examined by the T7EI assay, and the indel frequency ranged from ~20% to ~35%. All five mutants exhibited sharp and clear cleavage products (Fig. 5B), indicative of mutagenesis at the targeted locus. Sequencing results revealed that six of 15 clones (40%) had indel mutations from one 4<sup>th</sup> instar larva (Fig. 5C, b). Consequently, the CRISPR/Cas9 system effectively induced mutagenesis at the *Pxabd-A* locus in the genome.

#### 3.5. Germline transformation mediated by CRISPR/Cas9

A total of 23 somatic mutated males and 51 females, survived to the adult stage. Each of these mutants was outcrossed to wild-type

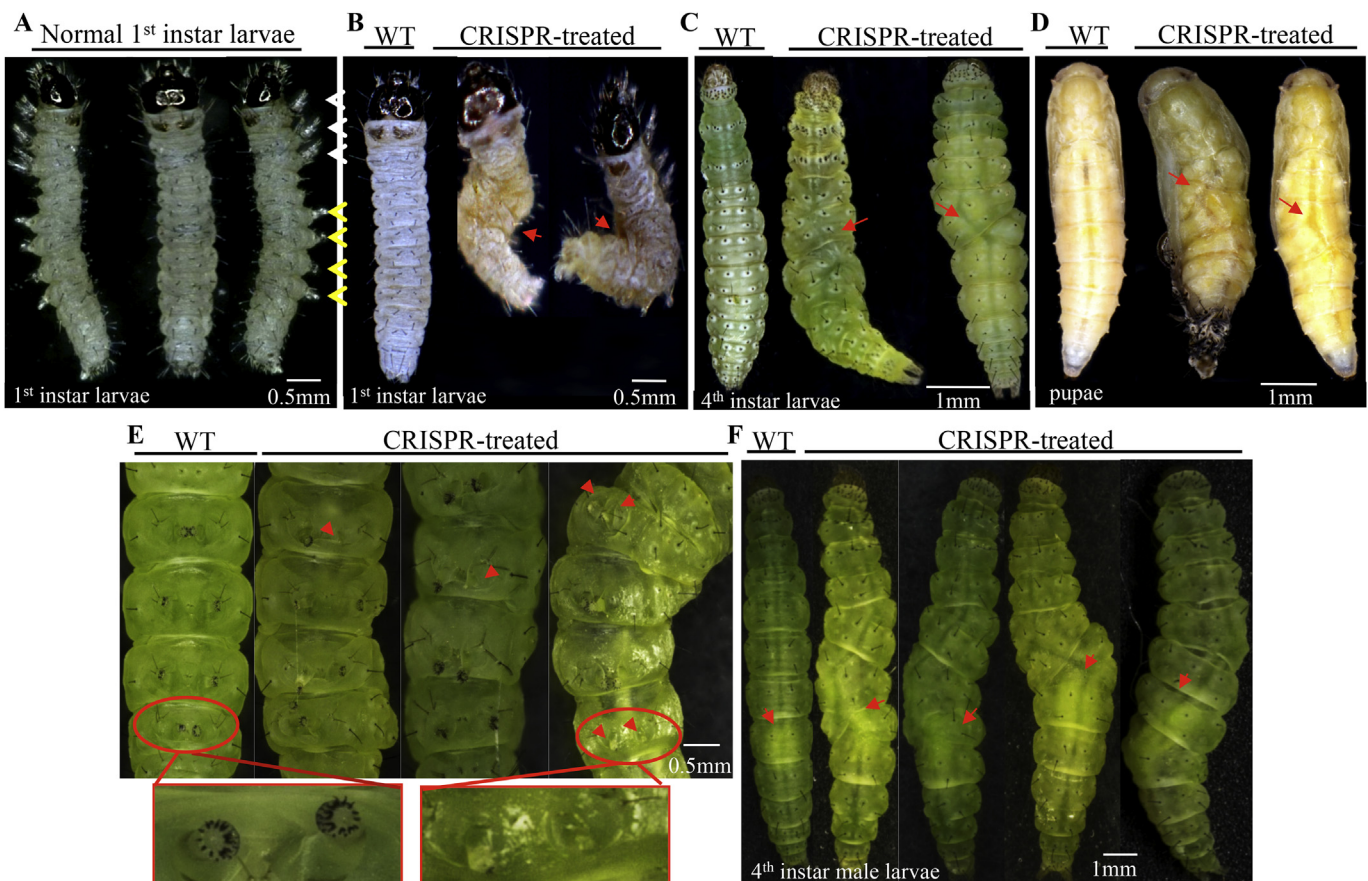


**Fig. 3. Phenotypes of *Pxabd-A* G<sub>0</sub> chimeric mutants.** (A) Wild-type 1<sup>st</sup> instar larvae of *P. xylostella* showing three pairs of thoracic appendages located on the thoracic segments (T1-3, white arrowheads) and four abdominal appendages on four of the nine abdominal segments (A1-10, yellow arrowheads); (B), (C) and (D) shows disorder of body in 1<sup>st</sup> instar larvae (red arrowheads), 4<sup>th</sup> instar larvae and pupae, respectively. Wild-type: WT; CRISPR-treated means disruption of *Pxabd-A* individuals; (E) The difference of prolegs between WT and G<sub>0</sub> mutants. The red arrows signify the black crochet disappeared from some prolegs in CRISPR-treated mutants; (F) Illustration for formed testis in A5-A6 abdominal segments of the 4<sup>th</sup> instar male larvae. The red arrows show the position of testis. The wild-type testis of larvae is bacilliform mainly presenting in A5 and potentially extending to A6. CRISPR-treated male larvae show defective shapes of testis.

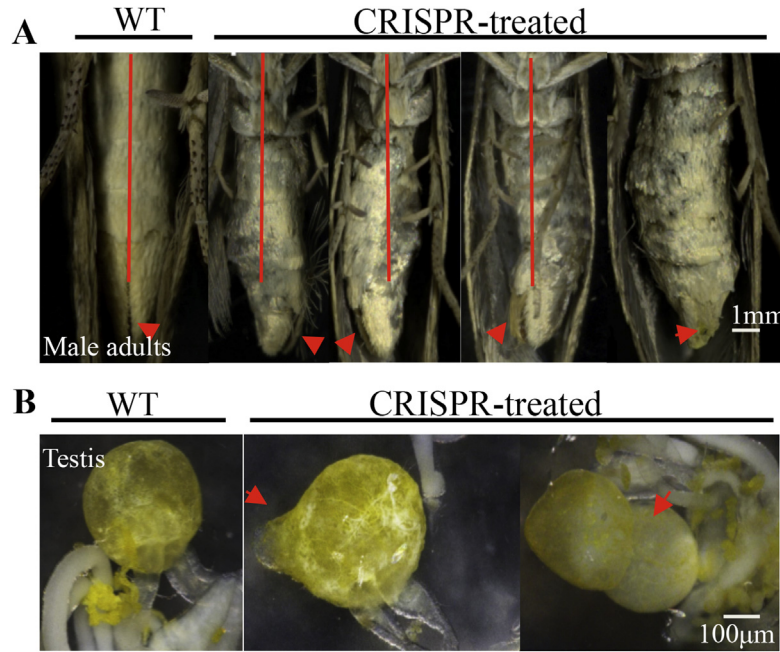


**Fig. 4. CRISPR-treated male adults were sterile and abnormal genitals.** (A) The external genitalia of wildtype and  $G_0$  mutated male adults. The red arrows indicate that the external genitalia of all mutated males were deviated from the original location; (B) The internal genitalia (testis) were highly abnormal. Testis of the wildtype male shows one regularly spheroidal (left lane). The red arrows indicate that irregular spherical testis (middle lane) in CRISPR-treated males, and some have two spheroidal testes (right lane).

adults. The genetically transformed mutants among generation 1 ( $G_1$ ) larvae were easily distinguishable based on the disorder of abdominal segments (Fig. 6A). Seven abnormal larvae were obtained following screening of 2,860  $G_1$  larvae from 33 egg batches. One abnormal  $G_1$  larva exhibited hardening in the A4–A8 abdominal segments and loss of abdominal mobility (Movie. 2). Six  $G_1$

mutated larvae exhibited phenotypes similar to those of  $G_0$  larvae (Fig. 6B). All  $G_1$  eggs laid by the wild-type females that had mated with mutated  $G_0$  males desiccated and did not hatch (Fig. 6C), consistent with them being unfertilized. To verify the mutagenesis of *Pxabd-A* locus in  $G_1$  larvae, we used DNA from a single individual as a template to perform direct PCR. Amplified fragments were

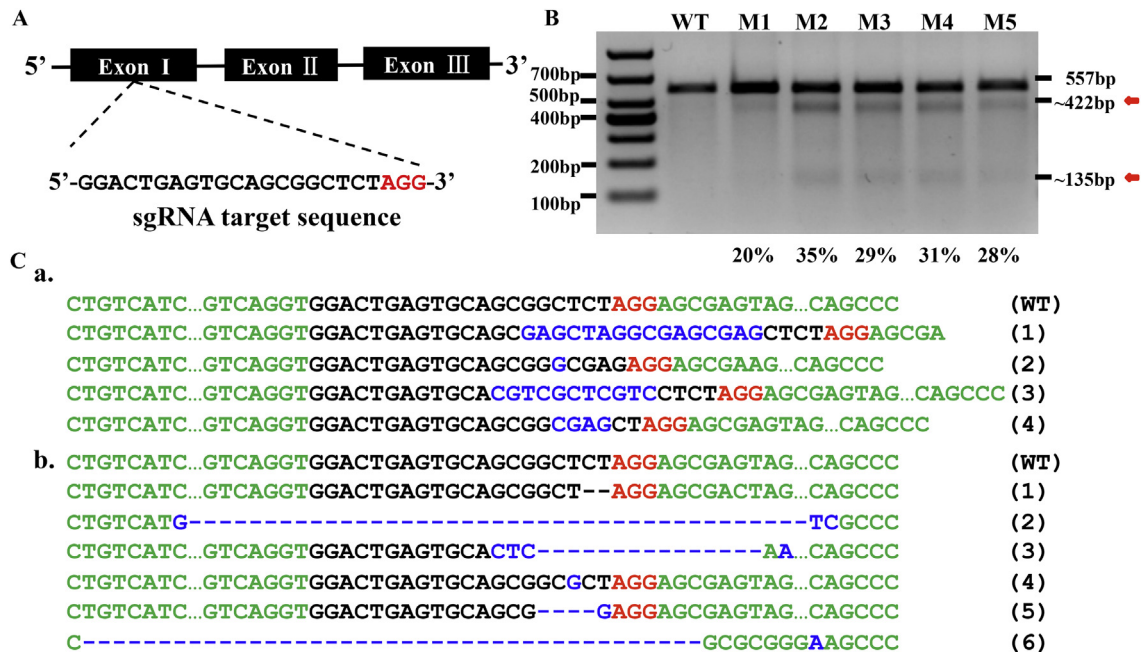


**Fig. 5. CRISPR/Cas9-induced mutations.** (A) Schematic representation of the sgRNA sequence targeted in Exon I of *Pxabd-A* locus; (B) Cleavage events and cutting efficiency were evaluated with a T7E1 assay. The T7E1 assays of five individual mutants are presented in lanes M1–5. The second lane is the control fragment (wild-type, WT) alongside the DNA marker. The digestion products (~422 bp and ~135 bp) are highlighted with red arrows. The percentage represents numerical brightness of the fragments based on the software of quantity one; (C) Mutation events confirmed by sequencing include both small deletions and insertions at specific sites, and at least three different types of mutations were found. Letters (a and b) represent mutated events of unhatched eggs and larvae, respectively. Sequences are of the sgRNA site (wild-type, WT) and four induced mutations (1–6). Sequences of the sgRNA target site are lettered in black, the PAM motif in red, and the insertions/deletions in blue.



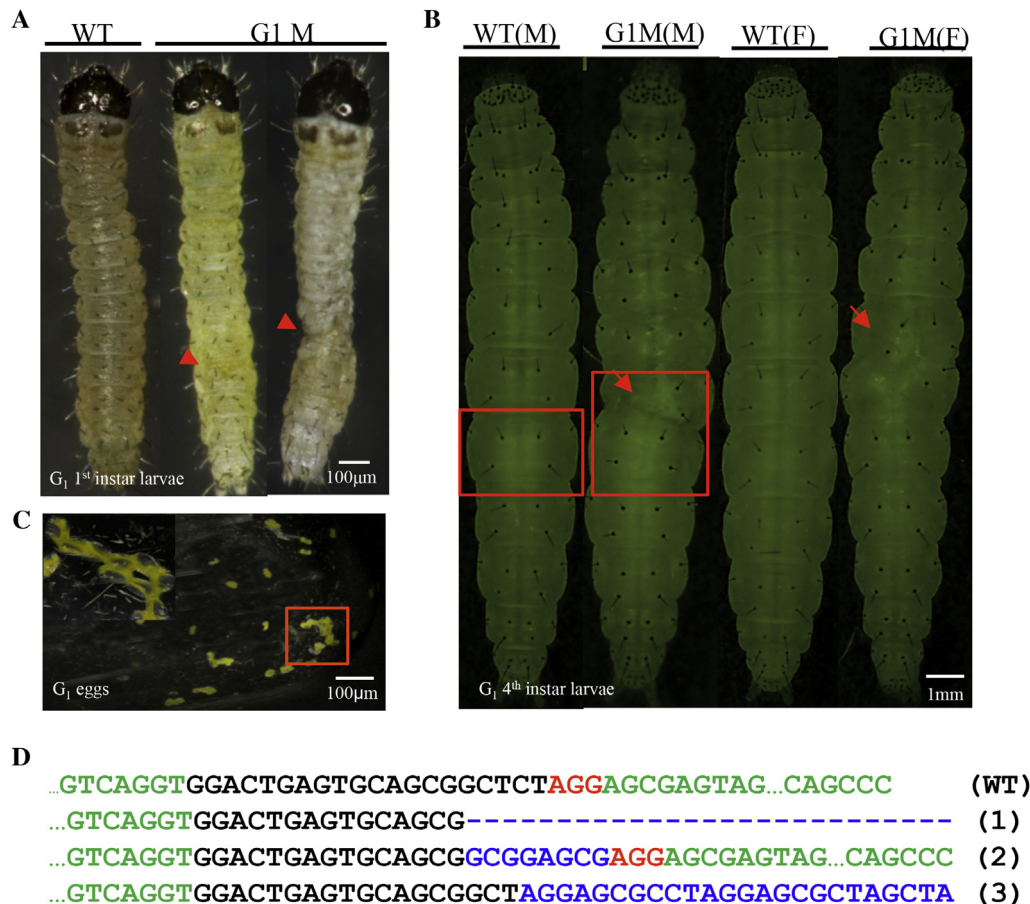


**Fig. 6. Phenotypes and genotypes of  $G_1$  mutants.** (A) The disorder of abdominal segments in  $G_1$  mutants, Wild-type: WT, Generation 1 mutants:  $G_1M$ ; (B) The male and female mutated  $G_1$  larvae. The red arrows signify the disorder segments of  $G_1$  mutants. The red squares highlight the region of the testis. WT(M): wild-type male larva;  $G_1M(M)$ :  $G_1$  mutated male larva; WT(F): wild-type female larva;  $G_1M(F)$ :  $G_1$  mutated female larva. (C) Eggs from wild type females mated with mutated males were desiccated. (D) Genotypes in  $G_1$  mutants. Fragment deletions and few base pair deletions are shown. Sequences are of the sgRNA targeted region (wild-type, WT) and three mutations (1–3). Sequences of the sgRNA target site are lettered in black, the PAM motif in red, and the insertions/deletions in blue.

cloned into vector and sequenced. Sequencing results showed that the mutated allele of  $G_1$  mutations exhibited deletion and insertion surrounding the targeted region of the *Pxabd-A* locus (Fig. 6D). The germline transmission efficiency was calculated by screening 33 egg batches with three positive egg batches (9.1%) that has at least one larva showing mutated phenotype and genotype (Table 1). Taken together, our findings demonstrate that the phenotypes and mutagenesis induced by disruption of *Pxabd-A* with CRISPR/Cas9 are heritable, despite the low germline transmission efficiency caused by sterile mutant males and females.

Supplementary video related to this article can be found at <http://dx.doi.org/10.1016/j.ibmb.2016.06.004>.

#### 4. Discussion

We show here that the CRISPR/Cas9 system can be used for targeting genes in an agricultural pest. This system is demonstrated to induce a series of insertions and deletions in the *P. xylostella* *abd-A*. Our results also showed stable germline mutations mediated by the CRISPR/Cas9 system. The germline transmission rate was 9.1%, which is much lower than that described for CRISPR/Cas9 use in silkworm (35.6%) However the  $G_0$  mutant rate (91%) is consistent with that seen in the silkworm (94%–100%) (Wang et al., 2013). The apparent deficit in DBM germline transmission efficiency may be attributable to the high percentage of sterility in males and females

caused by loss-of-function of *Pxabd-A*. These results demonstrate that the Cas9/sgRNA can induce the intended mutagenesis in *P. xylostella*, and be used as a powerful tool for genome manipulation of this globally significant pest.

We chose the *abd-A* as a targeted gene since it is required for determining the correct identity of A2–A8 in *Drosophila*. A single mutated allele of *abd-A* disrupts gene expression causing a strong transformation of A2–A3 and a weaker transformation of A5–A7 towards A1; and mutations are homozygous embryonic lethal (Busturia et al., 1989; Karch et al., 1985). Disruption of *Pxabd-A* causes severe mutations: fusion and disorder of abdominal segments A3–A8 were observed in mosaic mutated DBM larvae, unlike the segment transformation reported in *Drosophila* (Busturia et al., 1989; Karch et al., 1985; Sánchez-Herrero et al., 1984). The *abd-A* gene also is required for proleg development in the silkworm and they are missing following RNAi-mediated ablation of *Bmabd-A* transcripts (Pan et al., 2009). In contrast, our data showed proleg abnormalities resulting from mutations in *Pxabd-A*. In the adult stage, the external and internal genitalia of mutated males were abnormal. Previous reports in *Drosophila* showed that gonad formation and development require the *abd-A* domain, especially in the somatic cells of the gonad (Cumberledge et al., 1992; Foronda et al., 2006). This may explain the sterile females recovered in our study. Clearly, the detailed mechanisms resulting in the defects observed following mutating or ablating *abd-A* products require

further analysis.

The *abd-A* genes play roles other than defining abdominal segment identities as evidenced by previous studies. It is common that most transcription factors (such as *abd-A*) serve multiple roles during development in insects. Therefore, the molecular mechanisms disrupted by *Pxabd-A* mutagenesis are too complicated to be completely revealed based on our present study. However, mutations of *Pxabd-A* were transmissible to G<sub>1</sub> progeny indicating the feasibility of the CRISPR/Cas9 system in non-model organisms. CRISPR/Cas9 mediated genome editing for *P. xylostella* gene function studies is still challenging because most genes are recessive so only homozygous mutants display phenotypes. Recently, the mutagenic chain reaction (MCR) technique based on CRISPR/Cas9 (Gantz and Bier, 2015) was shown to be efficient in converting heterozygous recessive mutations to a homozygous state and revealing mutant phenotypes. Furthermore, the method can be used to obtain transgenic insects carrying effector genes, which can be expanded in field populations for pest management (Gantz et al., 2015). *P. xylostella* is a worldwide agricultural pest that has developed resistance to multiple classes of insecticides. The simplicity and adaptability of CRISPR/Cas9 opens the door for revealing gene function and new avenues for management of this pest.

### Acknowledgements

We thank Anjian Tan, Jun Xu and Xien Cheng for reviewing the manuscript. We thank Rongmei Cheng, Huihui Liu, Lijun Cai, Xiaowei Li, Qun Liu and Honglun Bi for assistance in rearing insects and line up the embryos. This work was supported by National Natural Science Foundation of China (No. 31320103922 and No. 31230061) and a grant from the External Cooperation Program of BIC, Chinese Academy of Sciences (Grant No. GJHZ201305). AAJ is supported in part by a grant from the National Natural Science Foundation of China (PI YPH, 31420103918). GMG is supported by the National Thousand Talents Program in China (GDT20153600063) and the Advanced Talents of SAEFA.

### Appendix A. Supplementary data

Supplementary data related to this article can be found at <http://dx.doi.org/10.1016/j.ibmb.2016.06.004>.

### References

- Busturia, A., Casanova, J., Sanchez-Herrero, E., Gonzalez, R., Morata, G., 1989. Genetic structure of the *abd-A* gene of *Drosophila*. *Development* 107, 575–583.
- Cho, S.W., Kim, S., Kim, J.M., Kim, J.S., 2013. Targeted genome engineering in human cells with the Cas9 RNA-guided endonuclease. *Nat. Biotechnol.* 31, 230–232.
- Cong, L., Ran, F.A., Cox, D., Lin, S., Barretto, R., Habib, N., Hsu, P.D., Wu, X., Jiang, W., Marraffini, L.A., 2013. Multiplex genome engineering using CRISPR/Cas systems. *Science* 339, 819–823.
- Cumberledge, S., Szabad, J., Sakonju, S., 1992. Gonad formation and development requires the *abd-A* domain of the bithorax complex in *Drosophila melanogaster*. *Development* 115, 395–402.
- Deng, H., Zhang, J., Li, Y., Zheng, S., Liu, L., Huang, L., Xu, W.H., Palli, S.R., Feng, Q., 2012. Homeodomain POU and Abd-A proteins regulate the transcription of pupal genes during metamorphosis of the silkworm, *Bombyx mori*. *Proc. Natl. Acad. Sci.* 109, 12598–12603.
- Foronda, D., Estrada, B., de Navas, L., Sánchez-Herrero, E., 2006. Requirement of Abdominal-A and Abdominal-B in the developing genitalia of *Drosophila* breaks the posterior downregulation rule. *Development* 133, 117–127.
- Fraser Jr., M.J., 2012. Insect transgenesis: current applications and future prospects. *Annu. Rev. Entomol.* 57, 267–289.
- Friedland, A.E., Tzur, Y.B., Esvelt, K.M., Colaiácovo, M.P., Church, G.M., Calarco, J.A., 2013. Heritable genome editing in *C. elegans* via a CRISPR-Cas9 system. *Nat. Methods* 10, 741–743.
- Furlong, M.J., Wright, D.J., Dossdall, L.M., 2013. Diamondback moth ecology and management: problems, progress, and prospects. *Annu. Rev. Entomol.* 58, 517–541.
- Gantz, V.M., Bier, E., 2015. The mutagenic chain reaction: a method for converting heterozygous to homozygous mutations. *Science* 348, 442–444.
- Gantz, V.M., Jasinskiene, N., Tatarenkova, O., Fazekas, A., Macias, V.M., Bier, E., James, A.A., 2015. Highly efficient Cas9-mediated gene drive for population modification of the malaria vector mosquito *Anopheles stephensi*. *Proc. Natl. Acad. Sci.* 112, E6736–E6743.
- Gilbert, L.A., Larson, M.H., Morsut, L., Liu, Z., Brar, G.A., Torres, S.E., Stern-Ginossar, N., Brandman, O., Whitehead, E.H., Doudna, J.A., 2013. CRISPR-mediated modular RNA-guided regulation of transcription in eukaryotes. *Cell* 154, 442–451.
- Gratz, S.J., Cummings, A.M., Nguyen, J.N., Hamm, D.C., Donohue, L.K., Harrison, M.M., Wildonger, J., O'Connor-Giles, K.M., 2013. Genome engineering of *Drosophila* with the CRISPR RNA-guided Cas9 nuclease. *Genetics* 194, 1029–1035.
- Angkersmit, G.W., 1953. DDT resistance in *Plutella maculipennis* (Curt)(Lepidoptera) in Java. *Bull.* 44, 421–425.
- Johnson, D.R., 1953. *Plutella maculipennis* resistance to DDT in Java. *J. Econ. Entomol.* 46, 176–176.
- Karch, F., Weiffenbach, B., Peifer, M., Bender, W., Duncan, I., Celniker, S., Crosby, M., Lewis, E., 1985. The Abdominal Region of the Bithorax Complex. *Genes, Development and Cancer*. Springer, pp. 303–332.
- LaBeau, E.M., Trujillo, D.L., Cripps, R.M., 2009. Bithorax complex genes control alary muscle patterning along the cardiac tube of *Drosophila*. *Mech. Dev.* 126, 478–486.
- Li, D., Qiu, Z., Shao, Y., Chen, Y., Guan, Y., Liu, M., Li, Y., Gao, N., Wang, L., Lu, X., 2013. Heritable gene targeting in the mouse and rat using a CRISPR-Cas system. *Nat. Biotechnol.* 31, 681–683.
- Lovato, T.L., Nguyen, T.P., Molina, M.R., Cripps, R.M., 2002. The Hox gene abdominal-A specifies heart cell fate in the *Drosophila* dorsal vessel. *Development* 129, 5019–5027.
- Marchetti, M., Fanti, L., Berloco, M., Pimpinelli, S., 2003. Differential expression of the *Drosophila* BX-C in polytene chromosomes in cells of larval fat bodies: a cytological approach to identifying in vivo targets of the homeotic Ubx, Abd-A and Abd-B proteins. *Development* 130, 3683–3689.
- Martins, S., Naish, N., Walker, A., Morrison, N., Scaife, S., Fu, G., Dafa'alla, T., Alphey, L., 2012. Germline transformation of the diamondback moth, *Plutella xylostella* L., using the piggyBac transposable element. *Insect Mol. Biol.* 21, 414–421.
- Mathies, L.D., Kerridge, S., Scott, M.P., 1994. Role of the teashirt gene in *Drosophila* midgut morphogenesis: secreted proteins mediate the action of homeotic genes. *Development* 120, 2799–2809.
- Michelson, A.M., 1994. Muscle pattern diversification in *Drosophila* is determined by the autonomous function of homeotic genes in the embryonic mesoderm. *Development* 120, 755–768.
- Miller, J.C., Holmes, M.C., Wang, J., Guschin, D.Y., Lee, Y.L., Rupniewski, I., Beausejour, C.M., Waite, A.J., Wang, N.S., Kim, K.A., 2007. An improved zinc-finger nuclease architecture for highly specific genome editing. *Nat. Biotechnol.* 25, 778–785.
- Miller, J.C., Tan, S., Qiao, G., Barlow, K.A., Wang, J., Xia, D.F., Meng, X., Paschon, D.E., Leung, E., Hinkley, S.J., 2011. A TALE nuclease architecture for efficient genome editing. *Nat. Biotechnol.* 29, 143–148.
- Pan, M.H., Wang, X.Y., Chai, C.L., Zhang, C.D., Lu, C., Xiang, Z.H., 2009. Identification and function of Abdominal-A in the silkworm, *Bombyx mori*. *Insect Mol. Biol.* 18, 155–160.
- Pavlopoulos, A., Akam, M., 2011. Hox gene Ultrabithorax regulates distinct sets of target genes at successive stages of *Drosophila* haltere morphogenesis. *Proc. Natl. Acad. Sci.* 108, 2855–2860.
- Peifer, M., Karch, F., Bender, W., 1987. The bithorax complex-control of segmental identity. *Genes & Dev.* 1, 891–898.
- Peng, L., Zou, M., Ren, N., Xie, M., Vasseur, L., Yang, Y., He, W., Yang, G., Gurr, G.M., Hou, Y., 2015. Generation-based Life Table Analysis Reveals Manifold Effects of Inbreeding on the Population Fitness in *Plutella xylostella*. *Scientific reports* 5.
- Perrin, L., Monier, B., Ponzelli, R., Astier, M., Semeriva, M., 2004. *Drosophila* cardiac tube organogenesis requires multiple phases of Hox activity. *Dev. Biol.* 272, 419–431.
- Ponzelli, R., Astier, M., Chartier, A., Gallet, A., Théron, P., Sémériva, M., 2002. Heart tube patterning in *Drosophila* requires integration of axial and segmental information provided by the Bithorax Complex genes and hedgehog signaling. *Development* 129, 4509–4521.
- Porteus, M.H., Baltimore, D., 2003. Chimeric nucleases stimulate gene targeting in human cells. *Science* 300, 763–763.
- Qi, L.S., Larson, M.H., Gilbert, L.A., Doudna, J.A., Weissman, J.S., Arkin, A.P., Lim, W.A., 2013. Repurposing CRISPR as an RNA-guided platform for sequence-specific control of gene expression. *Cell* 152, 1173–1183.
- Rogers, W.A., Grover, S., Stringer, S.J., Parks, J., Rebeiz, M., Williams, T.M., 2014. A survey of the trans-regulatory landscape for *Drosophila melanogaster* abdominal pigmentation. *Dev. Biol.* 385, 417–432.
- Sánchez-Herrero, E., Vernós, I., Marco, R., Morata, G., 1984. Genetic organization of *Drosophila* bithorax complex. *Nature* 313, 108–113.
- Sander, J.D., Dahlborg, E.J., Goodwin, M.J., Cade, L., Zhang, F., Cifuentes, D., Curtin, S.J., Blackburn, J.S., Thibodeau-Beganny, S., Qi, Y., 2011. Selection-free zinc-finger-nuclease engineering by context-dependent assembly (CoDA). *Nat. Methods* 8, 67–69.
- Tabashnik, B.E., Cushing, N.L., Finson, N., Johnson, M.W., 1990. Field development of resistance to *Bacillus thuringiensis* in diamondback moth (Lepidoptera: Plutellidae). *J. Econ. Entomol.* 83, 1671–1676.
- Wang, Y., Li, Z., Xu, J., Zeng, B., Ling, L., You, L., Chen, Y., Huang, Y., Tan, A., 2013. The CRISPR/Cas system mediates efficient genome engineering in *Bombyx mori*. *Cell*



- Res. 23, 1414–1416.
- Wood, A.J., Lo, T.W., Zeitler, B., Pickle, C.S., Ralston, E.J., Lee, A.H., Amora, R., Miller, J.C., Leung, E., Meng, X., 2011. Targeted genome editing across species using ZFNs and TALENs. *Science* 333, 307–307.
- You, M., Yue, Z., He, W., Yang, X., Yang, G., Xie, M., Zhan, D., Baxter, S.W., Vasseur, L., Gurr, G.M., 2013. A heterozygous moth genome provides insights into herbivory and detoxification. *Nat. Genet.* 45, 220–225.
- Zalucki, M.P., Shabbir, A., Silva, R., Adamson, D., Shu-Sheng, L., Furlong, M.J., 2012. Estimating the economic cost of one of the world's major insect pests, *Plutella xylostella* (Lepidoptera: Plutellidae): just how long is a piece of string? *J. Econ. Entomol.* 105, 1115–1129.